Supplementary Information (SI) for Chemical Science.
This journal is © The Royal Society of Chemistry 2024

# Carbon-Based Bifunctional Heterogeneous Enzyme: Toward Sustainable Pollution Control

Yuting Sun[1a], Ming Guo[*1b], Shengnan Hu[b], Yankun Jia[b], Wenkai Zhu[b*], Yusuke Yamauchi[*c], Chaohai Wang[*d]

[a] College of Environmental and Resource Sciences, Zhejiang Agricultural & Forestry University, Hangzhou, Zhejiang 311300, China

[b] College of Chemistry and Materials Engineering, Zhejiang Agricultural & Forestry University, Hangzhou, Zhejiang 311300, China

[c] School of Chemical Engineering & Australian Institute for Bioengineering and Nanotechnology (AIBN), The University of Queensland Brisbane, Queensland 4072, Australia.

[d] Henan International Joint Laboratory of Green Low Carbon Water Treatment Technology and Water Resources Utilization, School of Municipal and Environmental Engineering, Henan University of Urban Construction, Pingdingshan, Henan 467036, China

* E-mail: guoming@zafu.edu.cn (Dr. Guo); E-mail: chaohai@huuc.edu.cn (Prof. C. Wang); E-mail: y.yamauchi@uq.edu.au (Prof. Y. Yamauchi)

1 The author contributed equally to this study.

## 1. Experimental Section

### 1.1 Chemical

Multi-Walled Carbon Nanotubes (MWCNTs), Acrylamide (AM), 3-Aminopropyltriethoxysilane (APTES), Glutaraldehyde (50%), Ethylene methacrylate (EDGMA), 2,2'-Azobis(2-methylpropionitrile) (AIBN) were purchased from Aladdin (Shanghai, China); Di(2-ethylhexyl) phthalate (DEHP), Dimethyl phthalate (DMP), Di-n-octyl phthalate (DnOP), Di-iso-decyl phthalate (DIDP), 4-nitrophenol palmitate (p-NPP), Bovine Serum Albumin (BSA) and Fluorescein isothiocyanate (FITC) were purchased from Sigma-Aldrich (Shanghai, China); Candida lipolytica lipase was purchased from Shifeng Biotechnology Ltd. (Shanghai, China). All other chemicals and solvents were of analytical reagent grade.

### 1.2 Instrumentation

Transmission electron microscopy (TEM) images were measured with a FEI Talos F200S electron microscope at an operating voltage of 297 kV. The sample was dispersed in a solvent and sonicated to make it uniformly dispersed, and the transmission electron microscope sample was made by dropping the sample suspension onto a copper grid to observe the morphological characteristics of the sample. Images were collected using a CCD camera mounted. Raman spectroscopy measurements were performed using a Renishaw inVia spectrometer with a 532 nm excitation laser line. The spectra were obtained with a scan range of 400 to 4000 $cm^{-1}$. The surface chemistry of the samples was probed by X-ray photoelectron spectroscopy (XPS) using a Thermo Scientific K-Alpha instrument. Nitrogen adsorption/desorption measurements were carried out on a Micromeritics ASAP 2460 analyzer at 77 K after the samples were degassed at 200°C for 8 h under vacuum. Fluorescence imaging photos were collected using fluorescence microscopy at 488 nm excitation on a Nikon Ts2-FL system. Electrochemical experiments were performed using a CHI660C electrochemical workstation with a standard three-electrode system. A bare or modified glassy carbon electrode (GCE) was used as the working electrode, a platinum wire was used as the counter electrode, and a saturated Ag/AgCl electrode was used as the reference electrode.

### 1.3 Optimization of the reaction conditions for the molecularly imprinted prepolymer

The ability of template molecule (DEHP) to bind functional monomers (MAA, MMA, and AM) was investigated using UV-Vis spectrophotometry. The most suitable functional monomers

and ratios were identified. The UV spectra of DEHP, MAA, MMA, and AM were first measured separately. Then DEHP was mixed with a solution of each of the three functional monomers separately and fixed with methanol. Polymerization was carried out in a refrigerator at 4°C for 12 h. Three DEHP–functional monomer solutions were obtained.

Next, the optimum ratio of the template molecule to the functional monomer was determined. The concentration of the functional monomer in the solution was changed while holding the DEHP concentration constant to prepare mixtures of functional monomers with the template molecules at various concentrations. DEHP was mixed with the functional monomers in molar ratios of 1:1, 1:2, 1:4, 1:6, 1:8, and 1:10. These mixtures were then fixed with methanol and stored at 4°C for 12 h. A UV-Vis spectrophotometer was used to scan the solutions between the wavelengths of 190 and 400 nm.

**1.4 Preparation of MIP-AMWCNTs**

The surface of the MWCNTs was oxidized by treatment with strong acid[1]. MWCNTs (1 g) were dissolved in a solution of $H_2SO_4$/$HNO_3$ (3:1, v/v), followed by continuous ultrasonic dispersion at 65°C for 4 h. The above dispersion was stirred in a water bath at 80°C for 24 h. After cooling to room temperature, the MWCNTs were separated by centrifugation and washed with double-distilled water until the washing solution was neutral. The MWCNTs were filtered through a 0.22-μm filter membrane and then dried for 24 h at 80°C in a drying oven. The acidified MWCNTs were labeled as MWCNTs-COOH. The MWCNTs-COOH (0.5 g) were added to 100 mL of toluene and the solution was soaking for 3 h to swollen them. After ultrasonic dispersion, an excess of APTES solution was added dropwise while stirring. The mixture was refluxed under $N_2$ protection at 60°C for 12 h. The solution was washed several times to remove impurities. After drying the APTES-MWCNTs were ground to obtain a powder, which was labeled as AMWCNTs. The template molecule (DEHP) and functional monomer (Acrylamide) were pre-polymerized in chloroform at a ratio of 1:4 to form a monomer–template molecule complex. The AMWCNTs dispersion and EDGMA were added for the cross-linking reaction. Finally, a small amount of AIBN was added. After ultrasonic dispersion, the anaerobic environment was maintained by bubbling with $N_2$. The reaction was carried out at 60°C for 24 h. The solid was isolated by filtration. Soxhlet extraction was performed with a mixture of methanol/acetic acid (4:1, v:v) as extractant to remove template molecules and impurities. The product was washed with methanol

until the solution was neutral and then vacuum dried to obtain the carbon-based molecularly imprinted functional units, which were labeled as MIP-AMWCNTs. Carbon-based blank molecularly imprinted functional units, labeled as NIP-AMWCNTs, where prepared using the same method but without the template.

**1.5 Preparation of MIP-AMWCNTs@lipase**

The structural stability of heterogeneous enzyme is significant. The cross-linking method both protects the activity and helps to form a stable structure. The MIP-AMWCNTs were dispersed in 4% glutaraldehyde solution, which was stirred for 12 h. The solution was then centrifuged and the MIP-AMWCNTs were washed to remove unreacted glutaraldehyde. Finally, the MIP-AMWCNTs were ultrasonically dispersed in lipase solution and stirred for 24 h at 4°C. After the reaction, the powder was washed with Tris-HCl buffer (pH 9.0) and the washing solution was collected. Freeze-drying overnight yielded a carbon-based bifunctional heterogeneous enzyme, which was labeled as MIP-AMWCNTs@lipase.

**1.6 Lipase activity assay**

The activities of free lipase and MIP-AMWCNTs@lipase were determined spectrophotometrically using *p*-NPP as a substrate using an established method[2]. The *p*-NPP is hydrolyzed by lipase to *p*-NP and turns a distinct yellow color, which allows for a convenient and visible assay. Tris-HCl buffer containing gum arabic (0.1%) and sodium deoxycholate (0.2%), *p*-NPP, and lipase solution were mixed sequentially in a volume ratio of 22:1:1. The solution was incubated in a thermoshaker at 40°C for 10 min. Trichloroacetic acid (10%) was used to terminate the reaction, and sodium carbonate (10%) was added to develop the color. The solution was after filtered through a membrane and then the absorbance was measured at 410 nm by a microplate reader. The lipase activity amounting to one unit was defined as the amount of lipase required to release 1 μmol of *p*-NP per minute under the above conditions.

The relative activity of the lipase was related to the corresponding highest activity (100% represents the highest activity), which was calculated as follows (Equation S1):

$$Relative\ activity\ (\%) = \frac{Residue\ Activity}{Origin\ Activity} \times 100\ \% \qquad (S1)$$

The buffers of different pH values (4.0–11.0) were used to determine the optimum pH of the lipase. To determine the optimum temperature of lipases, the activities were measured at different

temperatures (25°C–80°C). Lipase activity measured under the optimum conditions was recorded as 100%. The buffer systems used were 20 mmol·L$^{-1}$ sodium acetate-acetic acid buffer (pH=4.0-6.0), 20 mmol·L$^{-1}$ PBS buffer (pH=6.0-7.0), 20 mmol·L$^{-1}$ Tris-HCl buffer (pH=7.0-9.0) and 20 mmol·L$^{-1}$ glycine-NaOH buffer (pH=9.0-11.0).

**1.7 Determination of enzyme loading**

The Bradford[3] method with BSA as the protein standard was used to measure the initial concentration of protein and the final concentration of protein in the carrier. The loading efficiency was calculated by Equation S2.

$$Loading\ efficiency\ (\%) = \frac{C_0V_0 - C_1V_1}{C_0V_0} \times 100\% \qquad (S2)$$

where $C_0$ (mg·mL$^{-1}$) is the initial soluble lipase concentration, $V_0$ (mL) the initial lipase volume, $C_1$ (mg·mL$^{-1}$) is the protein content in the collected supernatant, and $V_1$ (mL) is the total volume of the collected supernatant.

The specific vitality was calculated using the following equation (Equation S3):

$$Specific\ activity\ (U{\cdot}mg^{-1}) = \frac{Intial\ activity\ of\ immobilized\ lipase}{Protein\ content\ of\ immobilized\ lipase} \qquad (S3)$$

FITC was used as a fluorescent probe to visualize the immobilization of the enzyme. In the presence of excitation light, fluorescently labeled enzyme emits green fluorescence and can be used for qualitative detection of enzymes. 1.25 mL of FITC (1 mg·mL$^{-1}$) dye solution was added to the lipase supernatant. The reaction was stirred at 4°C for 24 h, protected from light, so that the lipase molecules could be sufficiently bound to the FITC molecules. The reaction was terminated by adding $NH_4Cl$ to a final concentration of 50 mmol·L$^{-1}$. The FITC-stained finished lipase solution was dialyzed with a protein dialysis bag of 14 kDa for 36 h. This process was performed mainly to remove the FITC dye that was not bound to the lipase. During the dialysis process, the dialysate was replaced every 3 h, and the dialysis was completed after 36 h to obtain a pure FITC-stained lipase solution. MIP-AMWCNTs were immobilized with FITC fluorescently stained and dialyzed enzyme solution as described in "1.5 Preparation of MIP-AMWCNTs@lipase." to obtain

FITC-labeled MIP-AMWCNTs@lipase, denoted as MIP-AMWCNTs@lipase-FITC. Then it was dispersed in water and placed on a slide to record fluorescence microscopy images.

**1.8 Enzymatic reaction kinetics**

The enzymatic kinetics of lipases for different concentrations of substrates were determined under the optimum lipase activity conditions. The Lineweaver–Burk[4] double inverse plotting method was used to plot $1/[S]$–$1/V$ kinetic curves. The Michaelis–Menten[5] model was used to determine the kinetic parameters, including the Michaelis–Menten constant ($K_m$), maximum velocity ($V_{max}$), and turnover rate ($k_{cat}$) for free lipase and MIP-AMWCNTs@lipase. The Michaelis–Menten equation can be expressed as follows (Equation S4):

$$V = \frac{V_{max} \times [S]}{K_m + [S]} \qquad (S4)$$

$$k_{cat} = \frac{V_{max}}{[E_0]} \qquad (S5)$$

where $V$ (mmol·(L·min)$^{-1}$) is the rate of enzymatic reaction of the system, $[S]$ (mmol·L$^{-1}$) is the concentration of the substrate involved in the reaction, and $[E_0]$ (mM) is the concentration of lipase.

**1.9 Stability performance**

Stability is a crucial metric used in industry to assess the quality of heterogeneous enzymes. We tested thermal stability, pH stability, storage stability and reusability separately. Thermal stability was the residual activity measured when the sample was incubated at 60°C for a period of time. The pH stability was the residual activity measured after 12 h of incubation at constant temperature under different buffer conditions (pH=4.0-11.0). The buffer system used was the same as the optimal pH experiment. Storage stability was assessed after the samples were incubated at 4°C for 18 days. Reusability is a key indicator of the sustainable utilization of product quality. Under the optimal activity conditions, the same batch of lipases was subjected to 7 repetitions of activity tests to determine the reusability of the lipases. The initial enzyme activity was defined as 100% in all stability experiments.

**1.10 Synergistic effect of adsorption and degradation**

DEHP molecules readily aggregate near the nanocarrier by adsorption, and then effectively degraded by lipase[6]. DEHP removal by heterogeneous enzymes should occur by a synergistic

adsorption-degradation process[7]. Therefore, removal effect should be studied in stages. We investigated the adsorption behavior of the MIP-AMWCNTs and NIP-AMWCNTs to clarify the adsorption properties and selective recognition performance of the carrier. Equal amounts of the MIP-AMWCNTs and NIP-AMWCNTs were added to 50 mL of DEHP (5 mg·L$^{-1}$) solution. The containers were sealed, and the solutions were placed in a constant temperature shaking incubator and shaken. The absorbance was measured at set intervals. The adsorption volume and adsorption rate were calculated using Equations S6, S7. Three parallel control groups were set up for each set of experiments.

$$Q_e = \frac{(C_0 - C_e)}{m} \times V \quad (S6)$$

$$\alpha = \frac{C_0 - C_e}{C_0} \times 100\ \% \quad (S7)$$

where $Q_e$ (mg·g$^{-1}$) is the equilibrium adsorption volume, $V$ (mL) is the volume of adsorbent solution, $m$ (mg) is the mass of adsorbent, $\alpha$ (%) is the adsorption rate, $C_0$ (mg·L$^{-1}$) is the initial concentration of DEHP, and $C_e$ (mg·L$^{-1}$) is the equilibrium concentration of DEHP.

DMP, DnOP, and DIDP are PAEs similar in structure to DEHP. Like DEHP, they are widely found in the aqueous environment. The molecular weights of DMP, DnOP, and DIDP are 194, 391, and 447 Da, which are less than DEHP, equal to DEHP, and greater than DEHP, respectively. And they represent different molecular weight classes of PAEs. Thus, DMP, DnOP, and DIDP were selected as potential competitors for adsorption of DEHP to verify the selective recognition performance of functional units. The stress responsiveness of the functional units was evaluated using the imprinting factor (IF) and selectivity coefficient (SC). The larger the IF, the stronger the imprinting binding and the better the effect. When SC is < 1, it indicates that the functional units have specific selectivity for DEHP. A smaller value of SC indicates that the functional units are more selective for the target pollutants. The IF and SC were calculated using Equations S8-S10, respectively.

$$K_D = \frac{Q_e}{C_e} \quad (S8)$$

$$IF = \frac{K_{DM}}{K_{DN}} \quad (S9)$$

$$SC = \frac{K_{D(PAEs)}}{K_{D(DEHP)}} \quad (S10)$$

where $K_D$ is the static assignment factor, IF is the imprinting factor, $K_{DM}$ is the static assignment

factor of MIP-AMWCNTs to substrates, $K_{DN}$ is the static assignment factor of the NIP-AMWCNTs to substrates, SC is the selectivity coefficient of MIP-AMWCNTs or NIP-AMWCNTs, $K_{D(DEHP)}$ is the static assignment of MIP-AMWCNTs to substrates DEHP factor, and $K_{D(PAEs)}$ is the static assignment factor of MIP-AMWCNTs to other PAEs substrates.

DEHP solutions (5 to 40 mg·L$^{-1}$) were prepared to investigate the synergistic adsorption-degradation of MIP-AMWCNTs@lipase. Equal amounts of MIP-AMWCNTs@lipase were added to 50 mL aliquots of DEHP solutions with different concentrations. The samples were placed in a constant temperature oscillating incubator. The absorbance of the supernatant was measured at set intervals. Kinetic curves were plotted for the synergistic adsorption-degradation with different concentrations of DEHP against time. The removal rates of MIP-AMWCNTs@lipase for different concentrations of DEHP were calculated using Equation S11. Three parallel control groups were set up for each group of experiments.

$$Removal\ rate\ (\%) = \frac{C_0 - C_t}{C_0} \times 100\ \% \qquad (S11)$$

where $C_0$ is the initial concentration of DEHP, and $C_t$ is the residual concentration of DEHP.

## 3. Supplementary Figures

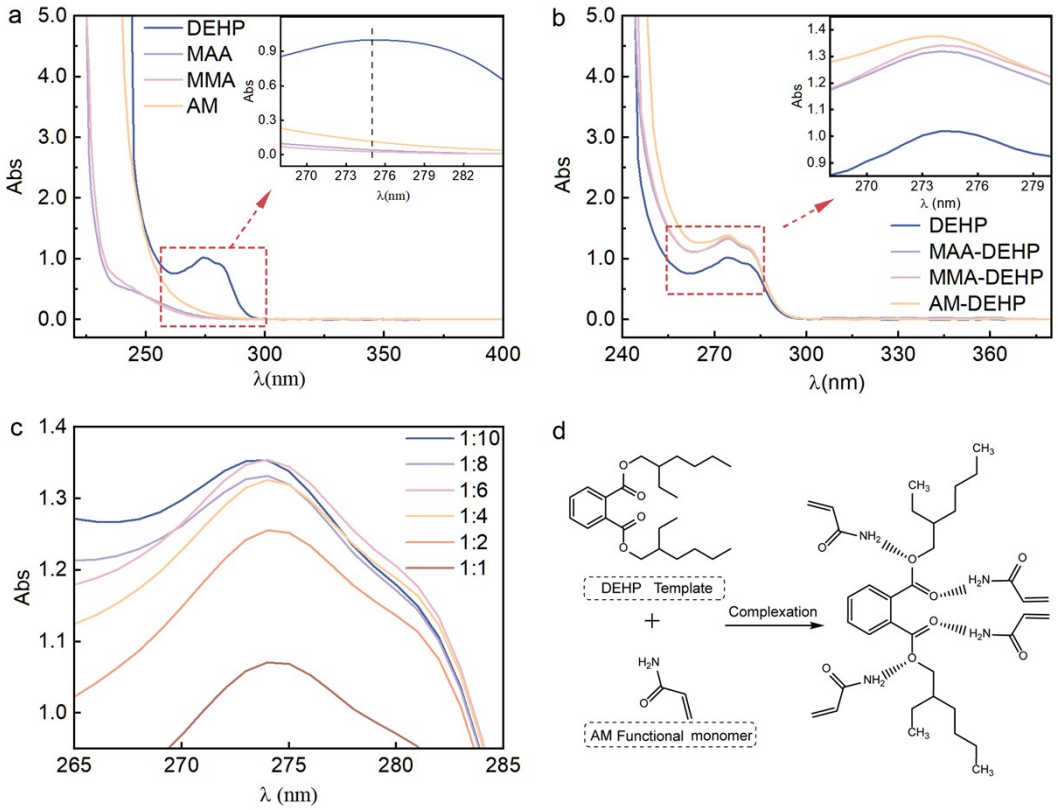


**Figure S1.** Optimization of the prepolymer reaction system: (a) UV absorption spectra of DEHP and three functional monomers; (b) UV absorption spectra of DEHP mixed with different functional monomer solutions; (c) UV absorption spectra of different ratios for the interaction between DEHP and AM; (d) schematic illustration of the interaction between DEHP and AM.

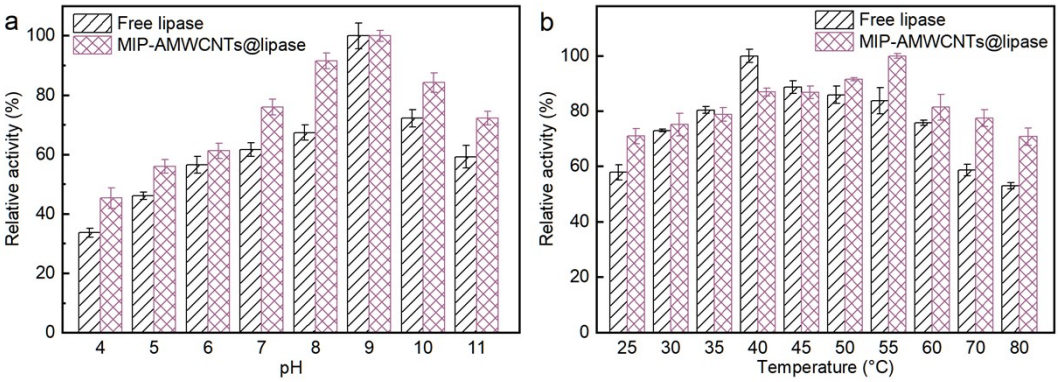


**Figure S2.** Enzymatic performance. (a) Effect of pH on lipase activity; (b) Effect of temperature on lipase activity

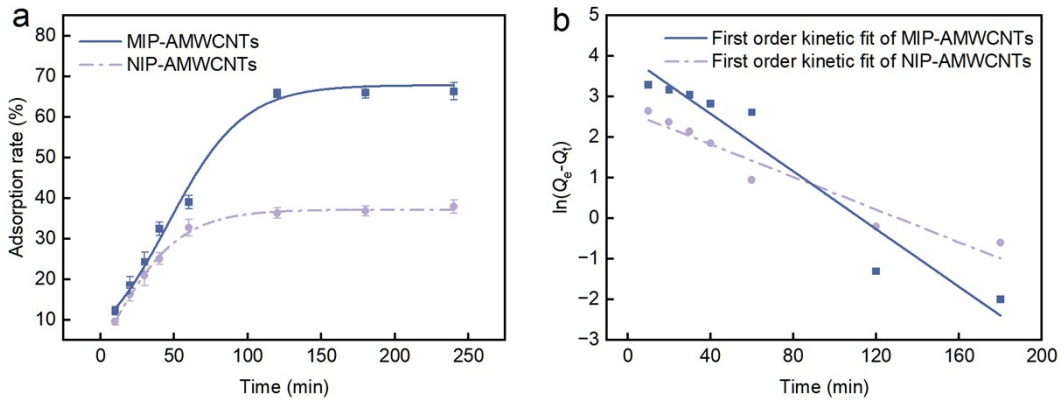


**Figure S3.** (a) The adsorption rates of MIP-AMWCNTs and NIP-AMWCNTs; (b) Pseudo-first-order kinetics fit of MIP-AMWCNTs and NIP-AMWCNTs

## 3. Supplementary Tables

**Table S1** Fitting details for the split C 1s peaks of MWCNTs-COOH and AMWCNTs

| MWCNTs-COOH | | | AMWCNTs | | |
|---|---|---|---|---|---|
| Binding Energy | The functional group | Content (%) | Binding Energy | The functional group | Content (%) |
| 284.8 | C=C $sp^2$ | 54.3 | 284.8 | C=C $sp^2$ | 46.3 |
| 285.5 | C-C $sp^3$ | 20.7 | 285.4 | C-C $sp^3$ | 32.4 |
| 286.6 | C-O | 10.8 | 286.4 | C-$NH_x$ | 9.9 |
| 288.9 | O-C=O | 9.1 | 288.8 | CON | 7.1 |
| 290.7 | π-π* | 5.1 | 291.0 | π-π* | 4.4 |

**Table S2** The pore structure parameters of samples

| Samples | Mean pore size (nm) | Surface area ($m^2 \cdot g^{-1}$) | Pore volume ($cm^3 \cdot g^{-1}$) |
|---|---|---|---|
| MIP-AMWCNTs | 26.5 | 204.8 | 1.6 |
| MIP-AMWCNTs@lipase | 28.3 | 134.6 | 1.0 |

**Table S3** Immobilization efficiency of different materials as carriers

| Support | Enzyme | Surface area ($m^2 \cdot g^{-1}$) | Immobilization efficiency | Ref. |
|---|---|---|---|---|
| Metal organic frameworks | Luciferase | 10.7 | 45% | [8] |
| Biochar | Lipase | 63.0 | 40%-60% | [9] |
| Mesoporous silica | L-ribose isomerase | 189.3 | 45% | [10] |
| Alumino-siloxane aerogels | Steapsin lipase | 192.0 | 41.40% | [11] |
| MIP-AMWCNTs | Lipase | 204.8 | 72.4% | This work |

**Table S4** Peak current and ratio, peak potential parameters of MIP-AMWCNTs@lipase at different scan speeds

| Scan rate (mV/ s) | $I_{pa}$ (μA) | $I_{pc}$ (μA) | $I_{pa}$ / $I_{pc}$ | $\Delta E_p$ (V) |
|---|---|---|---|---|
| 5 | 8.993 | 12.360 | 0.728 | 0.068 |
| 10 | 13.650 | 16.000 | 0.853 | 0.069 |
| 20 | 20.070 | 22.690 | 0.885 | 0.074 |
| 50 | 32.800 | 37.090 | 0.884 | 0.084 |
| 80 | 41.960 | 48.850 | 0.859 | 0.092 |
| 100 | 46.900 | 56.000 | 0.838 | 0.096 |
| 150 | 57.920 | 70.350 | 0.823 | 0.108 |
| 200 | 66.470 | 83.130 | 0.800 | 0.118 |
| 250 | 73.640 | 94.380 | 0.780 | 0.124 |
| 300 | 79.440 | 104.800 | 0.758 | 0.133 |

**Table S5** Enzymatic kinetics parameters of lipases

| Sample | $V_{max}$ (mmol·(L·min)$^{-1}$) | $K_m$ (mmol·L$^{-1}$) | $k_{cat}$ (min$^{-1}$) | $k_{cat}/K_m$ |
|---|---|---|---|---|
| Free lipase | $1.977\times10^{-3}$ | 0.907 | 0.652 | 0.719 |
| MIP-AMWCNTs @lipase | $4.846\times10^{-4}$ | 0.187 | 0.160 | 0.855 |

**Table S6** Kinetic parameters for degradation of DEHP by MIP-AMWCNTs@lipase

| Concentration | Equation | $k$ | $R^2$ |
|---|---|---|---|
| 5 mg·L$^{-1}$ | $y$=0.0120$x$+0.1000 | 0.0120 | 0.988 |
| 10 mg·L$^{-1}$ | $y$=0.0085$x$+0.0429 | 0.0085 | 0.999 |
| 20 mg·L$^{-1}$ | $y$=0.0064$x$-0.0688 | 0.0064 | 0.981 |
| 30 mg·L$^{-1}$ | $y$=0.0056$x$-0.0580 | 0.0056 | 0.982 |
| 40 mg·L$^{-1}$ | $y$=0.0048$x$-0.0694 | 0.0048 | 0.998 |

**References**


1. K. A. Wepasnick, B. A. Smith, K. E. Schrote, H. K. Wilson, S. R. Diegelmann and D. H. Fairbrother, *Carbon*, 2011, **49**, 24-36.
2. G. Pencreac'h and J. C. Baratti, *Enzyme Microb. Technol.*, 1996, **18**, 417-422.
3. L. Kielkopf Clara, W. Bauer and L. Urbatsch Ina, *Cold Spring Harb. Protoc.*, 2020, **2020**.
4. W. Khan, M. A. Abbasi, A. u. Rehman, S. Z. Siddiqui, M. Nazir, S. A. Ali Shah, H. Raza, M. Hassan, M. Shahid and S. Y. Seo, *J. Heterocycl. Chem.*, 2020, **57**, 2955-2968.
5. B. Choi, A. Rempala Grzegorz and K. J. Kyoung, *Scientific reports*, 2017, **7**, 1-11.
6. aW. Zhou, W. Zhang and Y. Cai, *Sep. Purif. Technol.*, 2022, **294**; bS. Ariaeenejad, E. Motamedi and G. H. Salekdeh, *Bioresour. Technol.*, 2022, **349**.
7. X. Du, L. Wang, Y. Li, J. Wu, G. Chen, H. Liang and D. Gao, *Int. Biodeterior. Biodegrad.*, 2023, **178**, 105564.
8. Z. Nowroozi-Nejad, B. Bahramian and S. Hosseinkhani, *Res. Chem. Intermed.*, 2019, **45**, 2489-2501.
9. M. E. Gonzalez, M. Cea, N. Sangaletti, A. Gonzalez, C. Toro, M. C. Diez, N. Moreno, X. Querol and R. Navia, *Journal of Biobased Materials and Bioenergy*, 2013, **7**, 724-732.
10. A. Singh and S. K. Yadav, *Journal of Biotechnology*, 2023, **362**, 45-53.
11. V. Linsha, K. A. Shuhailath, K. V. Mahesh, A. A. P. Mohamed and S. Ananthakumar, *Acs Sustainable Chemistry & Engineering*, 2016, **4**, 4692-4703.